

Comparison of Nonenhanced MR Angiographic Subtraction Techniques for Infragenual Arteries at 1.5 T: A Preliminary Study¹

Ruth P. Lim, MBBS, MMed, MS, FRANZCR
 Zhaoyang Fan, PhD
 Manjil Chatterji, MD
 Amanjit Baadh, MD
 Iliyana P. Atanasova, PhD
 Pippa Storey, PhD
 Danny C. Kim, MD
 Sooah Kim, MD
 Philip A. Hodnett, MD
 Afhsan Ahmad, MD
 David R. Stoffel, MR
 James S. Babb, PhD
 Mark A. Adelman, MD
 Jian Xu, MS
 Debiao Li, PhD
 Vivian S. Lee, MD, PhD, MBA

Purpose:

To evaluate diagnostic performance of three nonenhanced methods: variable-refocusing-flip angle (FA) fast spin-echo (SE)-based magnetic resonance (MR) angiography (variable FA MR) and constant-refocusing-FA fast SE-based MR angiography (constant-FA MR) and flow-sensitive dephasing (FSD)-prepared steady-state free precession MR angiography (FSD MR) for calf arteries, with dual-injection three-station contrast material-enhanced MR angiography (gadolinium-enhanced MR) as reference.

Materials and Methods:

This prospective study was institutional review board approved and HIPAA compliant, with informed consent. Twenty-one patients (13 men, eight women; mean age, 62.6 years) underwent calf-station variable-FA MR, constant-FA MR, and FSD MR at 1.5 T, with gadolinium-enhanced MR as reference. Image quality and stenosis severity were assessed in 13 segments per leg by two radiologists blinded to clinical data. Combined constant-FA MR and FSD MR reading was also performed. Methods were compared (logistic regression for correlated data) for diagnostic accuracy.

Results:

Of 546 arterial segments, 148 (27.1%) had a hemodynamically significant ($\geq 50\%$) stenosis. Image quality was satisfactory for all nonenhanced MR sequences. FSD MR was significantly superior to both other sequences ($P < .0001$), with 5-cm smaller field of view; 9.6% variable-FA MR, 9.6% constant-FA MR, and 0% FSD MR segmental evaluations had nondiagnostic image quality scores, mainly from high diastolic flow (variable-FA MR) and motion artifact (constant-FA MR). Stenosis sensitivity and specificity were highest for FSD MR (80.3% and 81.7%, respectively), compared with those for constant-FA MR (72.3%, $P = .086$; and 81.8%, $P = .96$) and variable-FA MR (75.9%, $P = .54$; and 75.6%, $P = .22$). Combined constant-FA MR and FSD MR had superior sensitivity (81.8%) and specificity (88.3%) compared with constant-FA MR ($P = .0076$), variable-FA MR ($P = .0044$), and FSD MR ($P = .0013$). All sequences had an excellent negative predictive value (NPV): 93.2%, constant-FA MR; 94.7%, variable-FA MR; 91.7%, FSD MR; and 92.9%, combined constant-FA MR and FSD MR.

Conclusion:

At 1.5 T, all evaluated nonenhanced MR angiographic methods demonstrated satisfactory image quality and excellent NPV for hemodynamically significant stenosis.

©RSNA, 2013

Supplemental material: <http://radiology.rsna.org/lookup/suppl/doi:10.1148/radiol.12120859/-/DC1>

¹From the Department of Radiology, New York University Medical Center, New York, NY (R.P.L., M.C., A.B., I.P.A., P.S., D.C.K., S.K., P.A.H., A.A., D.R.S., J.S.B.); Department of Radiology, Austin Health, 145 Studley Rd, Heidelberg, VIC 3084, Australia (R.P.L.); Department of Radiology, Cedars Sinai Hospital and UCLA Medical Center, Los Angeles, Calif (Z.F., D.L.); Department of Surgery, Division of Vascular Surgery, NYU Langone Medical Center, New York, NY (M.A.A.); Siemens Medical Solutions, New York, NY (J.X.); and Department of Radiology, University of Utah, Salt Lake City, Utah (V.S.L.). Received April 17, 2012; revision requested June 11; final revision received August 4; accepted September 19; final version accepted September 27. Address correspondence to R.P.L. (e-mail: ruth.lim@austin.org.au).

Peripheral arterial disease (PAD) affects approximately 8 million patients in the United States, with prevalence projected to increase as the population ages (1). Evaluation of the entire peripheral arterial tree is essential for revascularization planning, with gadolinium-enhanced magnetic resonance (MR) angiography or computed tomographic (CT) angiography as widely used noninvasive tests (2–5). CT angiography provides rapid,

high-spatial-resolution assessment, attractive where MR imaging is contraindicated by claustrophobia or implants (6). However, CT becomes less reliable where heavy arterial calcification is present (7) and places patients with renal impairment at risk for contrast material–induced nephrotoxicity (8), with renal impairment common in PAD (9). Contrast material–enhanced MR angiography is of concern in severe renal insufficiency, because of the risk of nephrogenic systemic fibrosis (10,11). A relatively rapid, reliable MR angiographic technique independent of gadolinium-based contrast material is desirable.

Two electrocardiographically triggered three-dimensional nonenhanced MR angiographic techniques have been described for peripheral arteries (12,13). With both techniques, arterial systolic data sets are subtracted from diastolic data sets, with arterial signal maintained during diastole but dephased during systole (Fig 1). The fast SE approach is commercially available and relies on systolic spin dephasing from fast arterial flow (13–16). Systolic arterial flow dephasing is paramount for accurate depiction of distal peripheral vessels and can be adjusted by altering the flip angle (FA) used to refocus transverse spins, with smaller FAs imparting greater sensitivity to slow flow (17). Incorporation of variable-refocusing FAs (18) (hereafter, variable FAs) increases

flow sensitivity over constant-refocusing FAs (hereafter, constant FAs), such that signal dephasing can be observed with velocities of 5 cm/sec (19).

Alternatively, a balanced SSFP-based technique employing FSD magnetization preparation to dephase intravoxel moving spins during systolic acquisitions only, which is not yet commercially available, has been proposed (12). With this approach, the higher the first-order moment of the applied FSD gradient pulses (m_1), the greater the systolic flow sensitivity (12).

Although both techniques have undergone preliminary human evaluation, their image quality and diagnostic accuracy have not been directly compared. Clear calf artery depiction is particularly important in diabetes or critical limb ischemia (2,20) and is dependent on time-resolved imaging or careful timing to avoid venous contamination with gadolinium-enhanced

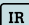

Advances in Knowledge

- Variable-refocusing–flip angle (FA) fast spin-echo (SE)–based MR angiography (variable-FA MR), constant-refocusing FA fast SE–based MR angiography (constant-FA MR), and flow-sensitive dephasing (FSD)–prepared steady-state free precession MR angiography (FSD MR) have excellent negative predictive values (NPVs) of 94.7% (593 of 626), 93.2% (643 of 690), and 91.7% (630 of 687), respectively, for hemodynamically significant ($\geq 50\%$) stenosis.
- A combination of FSD MR and constant-FA fast SE–based MR has the highest sensitivity (81.8%, 238 of 291) and specificity (88.3%, 695 of 787) for hemodynamically significant stenosis.
- Constant-FA MR angiography and FSD MR angiography are complementary; FSD MR angiography is preferable in patients with high flow states, such as ulcers or inflammation, or decreased flow, such as above-knee disease; constant-FA MR angiography allows a larger field of view for screening purposes where significant proximal disease is excluded, as it relies on good arterial inflow.
- Variable-FA fast SE–based MR angiography is less accurate in patients with elevated diastolic arterial velocities, including patients with foot ulceration.

Implications for Patient Care

- The relatively short acquisition time and high NPV of all assessed nonenhanced techniques supports their use as a safe screening and diagnostic tool, particularly in patients with renal impairment who are at risk for nephrogenic systemic fibrosis.
- FSD MR angiography or a combination of FSD MR angiography and constant-FA MR angiography can be used to provide robust assessment of infragrenal arterial disease over a range of disease states and arterial velocities at 1.5 T.

Published online before print

10.1148/radiol.12120859 Content codes:  

Radiology 2013; 276:293–304

Abbreviations:

ABI = ankle-brachial index
 FA = flip angle
 FOV = field of view
 FSD = flow-sensitive dephasing
 m_1 = first-order moment of the applied FSD gradient pulses
 NPV = negative predictive value
 PAD = peripheral arterial disease
 PDV = peak diastolic velocity
 PSV = peak systolic velocity
 SE = spin echo
 SSFP = steady-state free precession
 TD = trigger delay

Author contributions:

Guarantors of integrity of entire study, R.P.L., M.C.; study concepts/study design or data acquisition or data analysis/interpretation, all authors; manuscript drafting or manuscript revision for important intellectual content, all authors; approval of final version of submitted manuscript, all authors; literature research, R.P.L., Z.F., M.C., D.L., V.S.L.; clinical studies, R.P.L., Z.F., M.C., A.B., I.P.A., P.S., D.C.K., S.K., A.A., M.A.A., J.X.; statistical analysis, R.P.L., M.C., J.S.B.; and manuscript editing, R.P.L., Z.F., M.C., I.P.A., P.S., D.C.K., A.A., J.S.B., M.A.A., D.L., V.S.L.

Funding:

This research was supported by the National Institutes of Health (grants HL092439 and HL096119).

Conflicts of interest are listed at the end of this article.

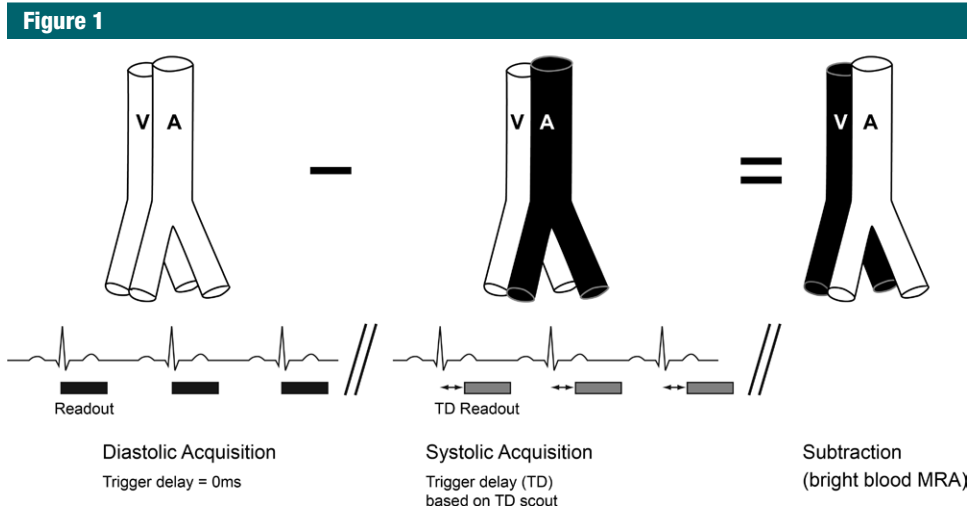


Figure 1: Basic sequence diagram depicting the principle underlying both electrocardiographically gated fast spin-echo (SE)-based MR angiography and flow-sensitive dephasing (FSD)-prepared steady state free precession (SSFP) MR angiography. Three-dimensional volumetric acquisitions in arterial diastole and arterial systole are obtained consecutively, with arterial signal intensity dephasing occurring during systole but not diastole. Subtraction of the systolic data set from the diastolic data set cancels out venous signal and static tissue, leaving only high arterial signal intensity. Scout phase-contrast imaging allows selection of the optimal systolic trigger delay (TD). A = artery, V = vein.

MR angiography (21). The purpose of our study was to evaluate clinical performance of variable-refocusing-FA fast SE-based MR angiography (hereafter, variable-FA MR angiography) and constant-refocusing-FA fast SE-based MR angiography (hereafter, constant-FA MR angiography) and FSD-prepared SSFP MR angiography (hereafter, FSD MR angiography) for calf arteries, with gadolinium-enhanced MR angiography as the reference standard.

Materials and Methods

One author (J.X.) is an employee of Siemens Medical Solutions (New York, NY), the manufacturer of the MR system used in this study. The remaining authors who are not employees of Siemens Medical Solutions (New York, NY) had control of inclusion of any data and information that might present a conflict of interest for this author. Two authors (J.X. and V.S.L.) have a patent pending on the variable-FA MR angiographic sequence.

Patients

This prospective study was institutional review board (NYU Langone

Medical Center, New York, NY) approved and Health Insurance Portability and Accountability Act compliant. After informed consent was obtained, lower-extremity MR angiography was performed in 21 consecutive patients (mean age, 62.6 years; range, 34–83 years), including 13 men (mean age, 61.5 years; range, 35–82 years) and eight women (mean age, 64.5 years; range, 34–83 years). Clinical indications were as follows: claudication ($n = 8$), rest pain ($n = 1$), foot ulceration ($n = 8$), suspected vascular malformation ($n = 3$), and neurofibromatosis ($n = 1$). Renal impairment and cardiovascular risk factors (known diabetes, hypertension, hyperlipidemia, current smoking, non-PAD cardiovascular disease, or family history of cardiovascular disease) were recorded (Table 1). Of 17 patients who had known PAD or who were suspected of having PAD, ankle-brachial index (ABI) was available in 16 patients, with a normal ABI (0.9–1.3) of the index leg in seven patients, and ABI of less than 0.9 in nine patients (mean, 0.57; range, 0.27–0.83). Abnormal ABI patient indications were rest pain ($n = 1$), nonhealing ulcer ($n = 1$), severe claudication at less than 200 m

Table 1

Renal Impairment and Known Cardiovascular Risk Factors in 21 Patients

Risk Factor	No. of Patients*
Renal impairment [†]	6 (29)
Diabetes	8 (38)
Hypertension	13 (62)
Hyperlipidemia	12 (57)
Current tobacco use	8 (38)
Family history of cardiovascular disease	2 (10)
Other cardiovascular disease [‡]	6 (29)

* Numbers in parentheses are percentages. Percentages were rounded

[†] Renal impairment was considered when the creatinine level was greater than 1.3 mg/dL (to convert to Système International units in micromoles per liter, multiply by 88.4).

[‡] Including coronary artery disease and ischemic cerebrovascular disease.

($n = 5$), and mild and/or moderate claudication ($n = 2$).

Imaging Protocol

Imaging was performed at 1.5 T (Avanto; Siemens Healthcare, Erlangen, Germany) with a 16-element peripheral

phased-array coil and additional coil elements from the six-element body matrix coil (anteriorly) and 24-element spine matrix coil (posteriorly) automatically selected by the MR system. Central electrocardiographic triggering was used, and heart rate and rhythm were recorded. Variable-FA MR angiography, constant-FA MR angiography, and FSD MR angiography were performed in random order before gadolinium-enhanced MR angiography in 17 of 21 patients (81%). Because of time constraints at the time of examination in the remaining subjects, nonenhanced MR angiographic sequences were performed separately after gadolinium-enhanced MR angiography, without intervention or clinical change between examinations (mean interval, 38 days; range, 2–117 days).

Systolic TD for all nonenhanced MR angiographic sequences was selected with an axial midcalf two-dimensional gradient-echo phase-contrast scout sequence (encoding velocity, 80 cm/sec), with time to peak systolic velocity (PSV) chosen for systolic TD (Mean Curve, Leonardo; Siemens Healthcare, Erlangen, Germany). If systolic TDs differed between legs, nonenhanced MR angiographic sequences were repeated with these TDs at the expense of time. A 0-msec TD was used for all nonenhanced MR angiographic diastolic acquisitions (Fig 1). For FSD MR angiography, a midcalf scout two-dimensional electrocardiographically gated SSFP sequence, with acquisition of images with increasing m_1 of 5–50 mT · msec²/m over 10 consecutive measures, was performed (22). The lowest m_1 at which complete arterial signal dephasing occurred was selected to minimize venous contamination, with repeat imaging if optimal m_1 differed between legs.

For variable-FA MR angiography, constant-FA MR angiography, and gadolinium-enhanced MR angiography, we used a 450-mm field of view (FOV) from tibial plateau to midfoot, with identical craniocaudal coverage. For FSD MR angiography, we used a 400-mm FOV to minimize off-resonance banding artifact, on the basis of prior experience (12). For all sequences, we used

parallel imaging with generalized auto-calibrating partially parallel acquisition and an acceleration factor of three (23). True voxel size ($1.4 \times 1.4 \times 1.9$ mm³) and total acquisition time (mean, 171 seconds for both systolic and diastolic acquisitions; range, 124–240 seconds) were matched for all nonenhanced sequences. Calf gadolinium-enhanced MR angiography was performed twice with identical positioning. First, time-resolved MR angiography with use of time-resolved imaging with stochastic trajectories (TWIST; Siemens Healthcare, Erlangen, Germany) was performed; this method is a view-sharing technique that employs a stochastic spiral trajectory to undersample k -space (21). Second, this technique was followed by imaging at the third station of a bolus-chase acquisition, with use of 0.15 mmol per kilogram body weight gadopentetate dimeglumine (Magnevist; Berlex Laboratories, Wayne, NJ) in total. Aortoiliac and femoral arteries were imaged as the first and second stations of the bolus-chase acquisition. Sequence parameters are summarized in Table 2. Figure E1 (online) shows details of the refocusing FA evolutions for fast SE-based MR angiography.

Image Analysis

Nonenhanced MR angiographic images were reviewed by two of four radiologists (A.A., S.K., P.A.H., D.C.K., with 1, 4, 6, and 9 years of MR angiography experience, respectively). Patients were randomly partitioned into four groups, and groups were randomly assigned to one of four distinct reader pairs, each consisting of one more experienced (6–9 years) and one less experienced (1–4 years) reader. Individual stenosis and image quality assessment of each anonymized nonenhanced MR angiographic data set (variable-FA MR angiography, constant-FA MR angiography, FSD MR angiography, combined constant-FA and FSD MR angiography) was performed by readers for their assigned patient groups in random order. Each patient was therefore evaluated by two independent readers with different levels of experience, and each reader evaluated approximately one-half of

the patients, permitting assessment of interreader agreement while maintaining reader effort at a reasonable level to avoid compromising data quality. Subtraction data sets were reviewed in random order with an independent workstation (Multimodality Workplace; Siemens Healthcare, Erlangen, Germany). During a later session, individual readers were presented with both constant-FA MR angiographic images and FSD MR angiographic images together, to obtain a combined assessment (constant-FA MR angiography and FSD MR angiography) for each assigned patient.

Thirteen segments were evaluated per leg: popliteal artery; tibioperoneal trunk; proximal, middle, and distal anterior tibial arteries, posterior tibial artery, and peroneal arteries; dorsalis pedis; and lateral plantar artery. Anterior tibial, posterior tibial, and peroneal arteries were divided into thirds, and arterial PSV and peak diastolic velocity (PDV) were measured in the TD scout sequence by a nonreader radiologist (R.P.L., with 5 years of vascular MR experience) with the same workstation mentioned above. Segmental image quality was assessed (score 0, unevaluable; score 1, poor; score 2, satisfactory; score 3, good), as were motion artifact, qualitative noise, and venous signal (score 1, none; score 2, mild; score 3, moderate; score 4, severe). Segmental stenosis was graded as follows: grade 0, no stenosis; grade 1, less than 50% stenosis; grade 2, one area of 50%–99% stenosis; grade 3, more than one area of 50%–99% stenosis; grade 4, occluded.

Reference standard was a consensus reading (all readers) of maximum intensity projection and source subtraction gadolinium-enhanced MR angiographic data sets for all patients, including all time-resolved MR angiographic phase data sets, with individual readings separated by at least 4 weeks. Conventional angiographic images were obtained in seven patients who subsequently underwent percutaneous intervention with a portable image intensifier (OEC 9900; GE Healthcare, Waukesha, Wis), without reported therapy or clinical change between MR angiography and conventional angiography (mean interval, 24

Table 2

Parameters for Variable-FA MR Angiography, Constant-FA MR Angiography, FSD MR Angiography, and Gadolinium-enhanced MR Angiography

Parameter	Variable-FA MR	Constant-FA MR	FSD MR	Gadolinium-enhanced MR	
				Time Resolved*	Bolus Chase†
Repetition time (msec)	1 R-R interval	1 R-R interval	1 R-R interval	3.1	3.1
Echo time (msec)	22	20	1.4	1.0	1.0
FA (degrees)	Variable	120	70	25	25
Echo spacing (msec)	2.4	2.8	3.1	NA	NA
Shots per section	2	2	2	NA	NA
Echo train length (echoes)	51	51	...	NA	NA
No. of segments	50	NA	NA
Data acquisition window (msec)	87	93	155	NA	NA
Bandwidth (Hz/pixel)	1042	1042	965	450	450
True voxel size (mm ³)	1.4 × 1.4 × 1.9	1.4 × 1.4 × 1.9	1.4 × 1.4 × 1.9	1.3 × 1.0 × 1.5	1.3 × 1.0 × 1.3
Acquisition time (sec)					
Mean total imaging time	171	171	171
Time per measure‡	17, full matrix; 5, partial matrix§	18
No. of measures	2	2	2	10	2
Partial Fourier					
Section	6/8	6/8	6/8	6/8	6/8
Phase	55%	55%	...	6/8	6/8
Restore magnetization pulse	On	On	On	NA	NA
Fat suppression	No	No	Yes	No	No
Contrast agent (mmol/kg)	NA	NA	NA	0.04	0.11

Note.— Further information in regard to variable FA evolution is detailed in Figure E1 (online) and reference 17. NA = not applicable.

* Time-resolved imaging was performed with time-resolved imaging with stochastic trajectories.

† Time-resolved imaging was followed by bolus-chase MR angiography, and parameters are provided for the third (calf) station.

‡ Values are for the first measure of gadolinium-enhanced MR angiographic sequences performed before contrast material was administered.

§ The time-resolved imaging with stochastic trajectories sampling factors were as follows: $A = 10\%$, $B = 25\%$, where A is center and B is periphery.

|| The contrast agent was gadopentetate dimeglumine.

days; range, 3–89 days). Conventional angiographic images were retrospectively interpreted by a vascular surgeon (M.A.A.), with 19 years of percutaneous interventional experience, who was blinded to the MR angiographic results. Conventional angiographic findings were not used as the reference standard in this subset but were correlated with the nonenhanced MR angiographic and the reference standard readings. Source data from patients with nondiagnostic image quality for nonenhanced MR angiographic images were reviewed by a non-reader radiologist (R.P.L.) after reader interpretations for causative factors.

Statistical Analysis

Only segments judged within the FOV by readers were included for analysis.

Mixed-model analysis of variance was used to compare pulse sequences for image quality and artifact scores. An “intent to diagnose” principle, whereby segments scored as nonevaluable were declared incorrect diagnoses, was used to evaluate sensitivity, specificity, and accuracy of nonenhanced MR angiographic sequences for hemodynamically significant ($\geq 50\%$) stenosis in comparison with reference results. Analysis was performed for all patients and was followed by a subanalysis excluding patients with overall image quality scores of zero for most segments in one or both legs.

Generalized estimating equations that were based on a binary logistic regression model were used to compare sequences for diagnostic accuracy relative to the reference standard, while

adjusting for any systematic reader differences (reader identity was included in the model as a blocking factor) and potential effects of subject-level factors (covariates) that might influence accuracy. Covariates were as follows: age, heart rate, rhythm (sinus or nonsinus), presence of cardiovascular risk factors, ejection fraction (available, $n = 11$), presence of hemodynamically significant ($\geq 50\%$) ipsilateral proximal above-knee stenosis, foot ulceration, and midcalf arterial PSV and PDV. Results were assumed to be correlated within patients and to be independent between patients. Interreader agreement was assessed with multireader κ coefficients. All reported P values are two sided, and significance was defined as a difference with a P value of less than .05. Software

(SAS 9.0; SAS Institute, Cary, NC) was used for all computations.

Results

With the reference standard, 148 of 546 (27.1%) segments had hemodynamically significant ($\geq 50\%$) stenosis. Segments were each evaluated by two readers, for 1092 total evaluations. Segments reported outside the FOV by readers were not evaluated further: 10 of 1092 (0.9%) evaluations for constant-FA MR angiography, 13 of 1092 (1.2%) for variable-FA MR angiography, and 32 of 1092 (2.9%) for FSD MR angiography (400-mm FOV).

Average heart rate was 66 beats per minute (range, 46–89 beats per minute), with sinus rhythm ($n = 17$), atrial fibrillation ($n = 3$), and frequent premature atrial contractions ($n = 1$). Diabetes (eight of 21 patients, 38.1%) and renal impairment (six of 21 patients, 28.6%) were relatively common.

Image Quality and Artifacts

Mean image quality scores were satisfactory for all nonenhanced sequences and were as follows: variable-FA MR angiography, 2.1 ± 1.0 (standard deviation); constant-FA MR angiography, 2.2 ± 0.9 ; FSD MR angiography, 2.4 ± 0.7 (scale of 0–3) (Figs 2, 3). Constant-FA MR angiographic image quality was significantly superior to variable-FA MR angiographic image quality, and FSD MR angiographic image quality was significantly superior to image quality for both variable- and constant-FA MR sequences ($P < .001$). Presence of above-knee significant stenosis negatively affected constant-FA MR angiographic image quality (2.1 vs 2.3, $P < .001$) and positively affected variable-FA MR angiography image quality (2.3 vs 2.0, $P < .001$), without having an effect on FSD MR angiographic image quality (2.4 for absent and present proximal disease).

Nondiagnostic image quality scores (score 0) were recorded for 104 of 1079 (9.6%) variable-FA MR angiographic evaluations. One hundred one of 104 segments were attributable to six of 42 legs in four of 21 patients (19%), with perceived motion artifacts observed

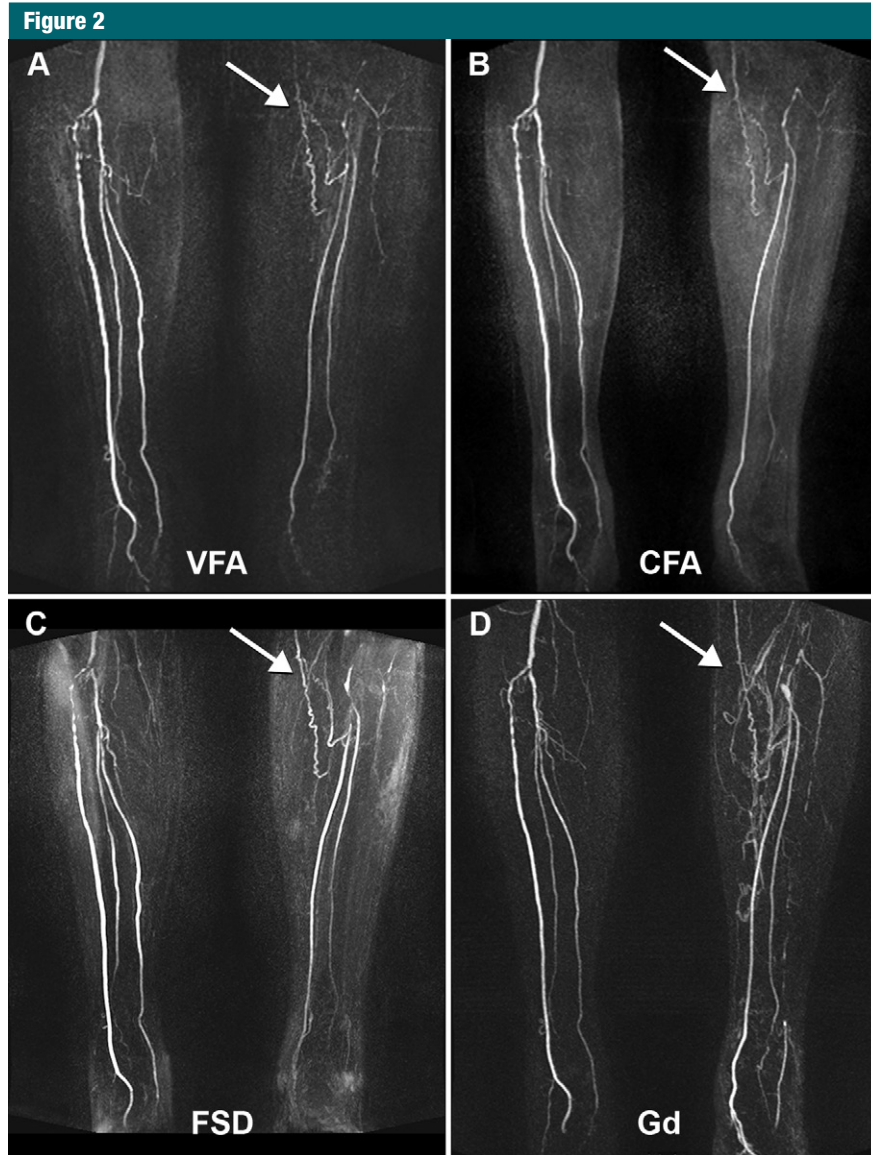


Figure 2: Claudication of left leg in 80-year-old man, with ABI of 0.6 in left leg and of 0.8 in right leg. *A*, Variable-FA (VFA) fast SE MR angiographic image. *B*, Constant-FA (CFA) fast SE MR angiographic image. *C*, FSD MR angiographic image. *D*, Time-resolved gadolinium (Gd)-enhanced MR angiographic image. Subtraction maximum intensity projection imaging depicts an occluded left popliteal artery with a medial collateral vessel (arrow) supplying the left calf arteries.

bilaterally and perceived image noise observed unilaterally in two patients each. Review of source variable-FA MR angiographic images scored as nondiagnostic demonstrated gross patency and diastolic signal dephasing because of high flow in four legs, attributed to motion and/or image noise. Nondiagnostic image quality scores noted for 104 of 1082 (9.6%) constant-FA MR

angiographic evaluations were caused by motion in two of 21 (10%) patients (four of 21 legs). No FSD MR angiographic evaluations were considered nondiagnostic (0%, 0 of 1060).

Median motion artifact scores (scale and range, scores 1–4) including nondiagnostic segments were as follows: variable-FA MR angiography, score 1; constant-FA MR angiography, score 2;

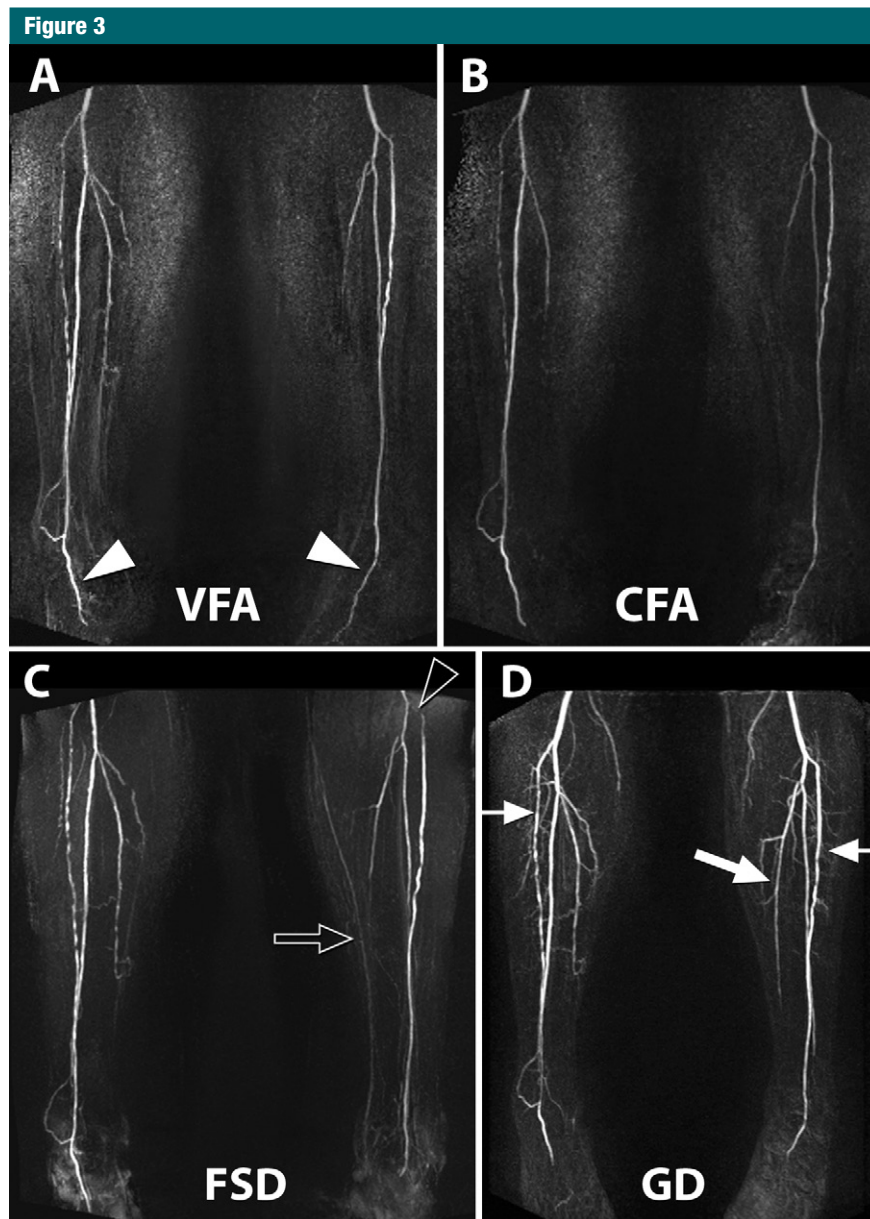


Figure 3: Rest pain of left leg in 71-year-old man with severe stenosis of left common iliac artery (not shown), with ABI of 0.5 in left leg and of 0.9 in right leg. *A*, Variable-FA (VFA) MR angiographic image. *B*, Constant-FA (CFA) MR angiographic image. *C*, FSD MR angiographic image. *D*, Gadolinium (GD)-enhanced MR angiographic image. *A–D*, Subtraction maximum intensity projection images depict disease involving the anterior tibial arteries bilaterally (thin arrows, *D*). The dorsalis pedis arteries bilaterally were well depicted with nonenhanced pulse sequences (arrowheads, *A*). A small-caliber midsegment of the distally occluded left posterior tibial artery (thick arrow, *D*) is not well shown in any of the sequences (PSV in the middle posterior tibial artery was 3.6 cm/sec). Minimal venous “contamination” is noted with FSD MR angiography, with the left long saphenous vein visible (arrow, *C*). Pseudostenosis of the left anterior tibial artery proximally (arrowhead, *C*) is also evident at FSD MR angiography, because of relative insensitivity to flow-dephasing gradient in the left-right direction (gradient was applied craniocaudally).

and FSD MR angiography, score 1. Subjective mean noise scores were similar

and were as follows: variable-FA MR angiography, 1.8 ± 0.9 ; constant-FA MR

angiography, 1.9 ± 0.8 ; and FSD MR angiography, 1.6 ± 0.7 . Minimal mean venous signal was as follows: variable-FA MR angiography, 1.1 ± 0.4 ; constant-FA MR angiography, 1.1 ± 0.4 ; and FSD MR angiography, 1.2 ± 0.5 . FSD MR angiography had significantly better scores for motion ($P = .19$) and noise ($P = .13$) and slightly worse venous contamination ($P = .88$) than the other sequences ($P < .0001$, all comparisons). There was no significant difference between variable-FA MR angiography and constant-FA MR angiography in regard to artifact scores.

Stenosis

Sensitivity and specificity for hemodynamically significant stenosis were not significantly different across the three approaches (Table 3). FSD MR angiography values were highest (sensitivity, 80.3% [232 of 289]; specificity, 81.7% [630 of 771]), compared with constant-FA MR angiography (sensitivity, 72.3% [214 of 296]; and specificity, 81.8% [643 of 786]) and variable-FA MR angiography (sensitivity, 75.9% [224 of 295]; and specificity, 75.6% [593 of 784]). Sensitivity (81.8%, 238 of 291) and specificity (88.3%, 695 of 787) were highest for combined constant-FA and FSD MR angiography, with specificity significantly higher than that of variable-FA MR angiography ($P = .004$), constant-FA MR angiography ($P = .008$), and FSD MR angiography ($P = .001$). Variable-FA MR angiography had the highest NPV (94.7%, 593 of 626), which was higher than the NPV of FSD MR angiography (91.7%, 630 of 687; $P = .03$) and approached significance with constant-FA MR angiography (93.2%, 643 of 690; $P = .052$). Positive predictive value was low for all nonenhanced MR angiographic sequences and was highest for combined constant-FA and FSD MR angiography (72.1%, 238 of 330).

When diagnostic-quality images (image quality, score of >0) were analyzed in 19 of 21 patients, constant-FA MR angiographic sensitivity (84.1%, 190 of 226), specificity (84.4%, 635 of 752), NPV (94.6%, 635 of 671), and accuracy (84.4%, 825 of 978) improved. Variable-FA MR angiographic results were similar; exclusion of four of 21

Table 3

Sequence Statistics for Depiction of Hemodynamically Significant Stenosis

Statistic	Variable-FA MR		Constant-FA MR		FSD MR		Combined Reading of Constant-FA and FSD MR Data Sets	
	Value (%)	95% CI	Value (%)	95% CI	Value (%)	95% CI	Value (%)	95% CI
Sensitivity	75.9 (224/295)	63.5, 82.5	72.3 (214/296)	54.0, 85.3	80.3 (232/289)	69.4, 88.0	81.8 (238/291)	71.6, 88.9
Specificity	75.6 (593/784)	65.9, 83.3	81.8 (643/786)	73.0, 88.2	81.7 (630/771)	73.2, 88.0	88.3 (695/787)*	81.4, 92.9
PPV	58.0 (224/386)	44.9, 70.1	62.9 (214/340)	52.6, 72.2	62.2 (232/373)	48.9, 73.9	72.1 (238/330)†	61.5, 80.7
NPV	94.7 (593/626)‡	91.0, 97.0	93.2 (643/690)	87.6, 96.4	91.7 (630/687)	84.5, 95.7	92.9 (695/748)	87.9, 96.0
Accuracy	75.7 (817/1079)	67.3, 82.5	79.2 (857/1082)	70.1, 86.1	81.3 (862/1060)	75.5, 86.0	86.5 (933/1078)	81.5, 90.4

Note.— Numbers in parentheses are the number of evaluations performed and were used to calculate the percentages. CI = confidence interval, NPV = negative predictive value, PPV = positive predictive value.

* Significantly superior to variable-FA MR angiography ($P = .004$), constant-FA MR angiography ($P = .008$), and FSD MR angiography ($P = .001$).

† Significantly superior to variable-FA MR angiography ($P = .02$), constant-FA MR angiography ($P < .01$), and FSD MR angiography ($P < .001$).

‡ Significantly superior to FSD MR angiography ($P = .03$).

patients with nondiagnostic image quality scores yielded sensitivity of 82.6% (157 of 190), specificity of 81.6% (560 of 686), NPV of 94.6% (560 of 592), and accuracy of 81.8% (717 of 876). No significant difference in accuracy of individual sequences was found in the subanalysis.

The multireader κ coefficient for interreader agreement was substantial for constant-FA MR angiography (0.63), FSD MR angiography (0.74), and combined constant-FA MR angiography and FSD MR angiography (0.68), with moderate interreader agreement for variable-FA MR angiography (0.50).

Effect of Covariates on Stenosis Assessment

Covariates are summarized in Table 4, with those significantly affecting stenosis evaluation discussed here. The presence versus absence of cardiovascular risk factors (Table 1) negatively affected variable-FA MR angiography (72.9%, 600 of 823, vs 84.8%, 217 of 256; $P = .03$) and constant-FA MR angiography accuracy (75.8%, 626 of 826, vs 90.2%, 231 of 256; $P = .003$). The presence versus absence of above-knee hemodynamically significant stenosis negatively affected constant-FA MR angiography accuracy (73.3%, 228 of 311, vs 87.5%, 629 of 719; $P = .01$). Slightly decreased variable-FA MR angiography ($P = .37$) and FSD MR angiography ($P = .59$) accuracy were not significant.

There was lower accuracy for heart rates of 63 beats per minute or less for constant-FA MR angiography (75.6%, 428 of 566, vs 83.1%, 429 of 516; $P = .03$) and FSD MR angiography (76.6%, 422 of 551, vs 86.4%, 440 of 509; $P = .03$). Of five patients with slower than normal sinus rhythm (< 60 beats per minute), two had atrial fibrillation and one had frequent premature atrial contractions. Midcalf PDV greater than 1.3 cm/sec (median value) was associated with significantly lower variable-FA MR angiographic accuracy, with 69.4% (68 of 98), versus 89.3% (100 of 112) for PDV of 1.3 cm/sec or less ($P = .02$) (Fig 4). In six of six legs where PDV was 5 cm/sec or greater, variable-FA MR angiography was unsuccessful, with poor or nondiagnostic image quality. Lower constant-FA MR angiography ($P = .076$) and minimally lower FSD MR angiography ($P = .62$) accuracy with higher PDV was not significant.

Conventional Angiography Correlation

Single-leg intraoperative conventional angiography was available in 77 segments in seven legs (Fig 4). Two segments (distal peroneal and plantar) were excluded because of angiography mistiming. In 33 of 75 segments (44%), hemodynamically significant stenosis was found at conventional angiography. In 60 of 75 segments (80%), the stenosis was concordant with findings at gadolinium-enhanced MR angiography,

with disease overestimation in 11 of 75 segments (15%) and underestimation in four of 75 segments (5.3%).

One hundred fifty segmental evaluations were performed (75 segments, two readers) per nonenhanced MR angiographic sequence. For variable-FA MR angiography, 149 of 150 segmental evaluations (99.3%) were considered within the imaging FOV, with 59 of 149 (39.6%) considered unevaluable, largely from perceived motion in three legs. In 58 of 90 evaluations (64.4%), findings were concordant with those of conventional angiography for hemodynamically significant stenosis, with underestimation in six of 90 (6.7%) and overestimation in 26 of 90 (28.9%) evaluations. For constant-FA MR angiography, 148 of 150 segmental evaluations (98.7%) were within the imaging FOV, with 13 of 148 (8.8%) scored unevaluable. In 78 of 135 evaluations (57.8%), findings were concordant with those at conventional angiography, with underestimation in six of 135 (4.4%) and overestimation in 51 of 135 (37.8%) evaluations.

For FSD MR angiography, 144 of 150 evaluations (96.0%) were within the imaging FOV, with no unevaluable image quality scores. FSD MR angiographic and conventional angiographic findings were concordant in 103 of 144 evaluations (71.5%), with underestimation in 10 of 144 (6.9%) and overestimation in 31 of 144 (21.5%) evaluations.

Table 4

Covariate Analysis: Accuracy Observed for Each Sequence When Results Are Stratified according to Specific Attributes

Factor, Stratifier, and P Value	Variable-FA MR Accuracy	Constant-FA MR Accuracy	FSD MR Accuracy
Age (y)			
≤67	77.4 (439/567)	79.4 (451/568)	83.0 (458/552)
>67	73.8 (378/512)	79.0 (406/514)	79.5 (404/508)
P value	.7	.31	.12
Heart rate (beats/min)			
≤63	72.9 (412/565)	75.6 (428/566)*	76.6 (422/551)*
>63	78.8 (405/514)	83.1 (429/516)*	86.4 (440/509)*
P value	.42	.03*	.03*
Sinus rhythm			
No	68.6 (140/204)	74.8 (151/202)	77.0 (154/200)
Yes	77.4 (677/875)	80.2 (706/880)	82.3 (708/860)
P value	.34	.35	.21
Cardiovascular risk factors			
Absent	84.8 (217/256)*	90.2 (231/256)*	85.8 (217/253)
Present	72.9 (600/823)*	75.8 (626/826)*	79.9 (645/807)
P value	.03*	.003*	.25
Ejection fraction (%) [†]			
≤60	78.0 (241/309)	74.7 (230/308)	81.0 (248/306)
>60	72.6 (223/307)	72.3 (224/310)	81.8 (247/302)
P value	.31	.87	.56
Above-knee ≥ 50% stenosis [‡]			
Absent	82.0 (578/705)	87.5 (629/719)*	82.0 (617/752)
Present	77.9 (239/307)	73.3 (228/311)*	79.5 (245/308)
P value	.37	.01*	.59
Ulcer			
Absent	83.2 (555/667)*	84.3 (565/670)	82.6 (545/660)
Present	63.6 (262/412)*	70.9 (292/412)	79.3 (317/400)
P value	.005*	.1	.53
PDV (cm/sec)			
≤1.3	89.3 (100/112)*	85.7 (96/112)	84.8 (95/112)
>1.3	69.4 (68/98)*	76.5 (75/98)	81.6 (80/98)
P value	.02*	.08	.62
PSV (cm/sec)			
≤18	80.6 (87/108)	73.1 (79/108)	79.6 (86/108)
>18	79.4 (81/102)	90.2 (92/102)	87.3 (89/102)
P value	.27	.35	.23

Note.—For age, the mean was 62.6 years (range, 34–83 years); for heart rate, the mean was 66 beats per minute (range, 46–89 beats per minute); for ejection fraction, the mean was 59.6% (range, 50%–68%); for PDV, the mean was 1.9 cm/sec (range, 0–14 cm/sec); and for PSV, the mean was 22.4 cm/sec (range, 1.7–146 cm/sec). For all other factors, these values were not applicable. For numeric attributes, results were stratified according to whether or not the attribute was less than or equal to the overall median value observed for that attribute. Accuracy data are percentages. Numbers in parentheses are numbers of evaluations performed and were used to calculate the percentages.

* Values indicate a significant difference.

[†] n = 11.

[‡] Hemodynamically significant ipsilateral proximal (above-knee) stenosis.

Discussion

Although several nonenhanced techniques have previously been described (12,14,15,24), they have not been

directly compared in patients. We evaluated two such techniques in a group that included patients with known PAD, diabetes, and foot ulceration. Both fast SE-based (variable-FA MR angiography

and constant-FA MR angiography) and FSD SSFP MR angiographic techniques were each completed in less than 4 minutes for calf MR angiography. No significant difference in diagnostic accuracy for hemodynamically significant stenosis was demonstrated between techniques. However, since sample size was not premised on statistical power, this lack of a significant difference may reflect inadequate statistical power. Therefore, interpretation of relative accuracy of the techniques should be guided by confidence intervals provided in Table 3. All techniques had excellent NPV, suggesting potential for completely noninvasive screening. They could be helpful in type 2 diabetes, where evaluation is challenging (25), and 71% sensitivity of ABI sensitivity for PAD has been reported (26), although addition of pulse volume recordings and toe pressure measurements can improve accuracy (25,27).

We identified several factors affecting individual sequence performance. Bulk motion was the most commonly perceived problem for both fast SE methods. High diastolic flow typically associated with ulceration (28) was most challenging for variable-FA MR angiography because of diastolic arterial signal dephasing leading to arterial nonvisualization (17,19,29).

For constant-FA MR angiography, although lower accuracy (73.1%, 79 of 108, vs 90.2%, 92 of 102) in patients with PSV of 18 cm/sec or less was not significant ($P = .35$), significantly lower accuracy was observed with proximal disease. This could be a result of incomplete systolic signal dephasing and cancellation of arterial signal on subtraction (29). Also, lower accuracy with high diastolic flow approached significance ($P = .08$). Our findings highlight the delicacy of appropriate constant-FA MR angiography refocusing-FA selection (17,19), which might benefit from a scout sequence similar to the m_1 scout sequence used for FSD MR angiography. For both variable-FA MR angiography and constant-FA MR angiography, accuracy was lower in patients with cardiovascular risk factors, perhaps from higher likelihood of arterial flow extremes. Subanalysis excluding patients with

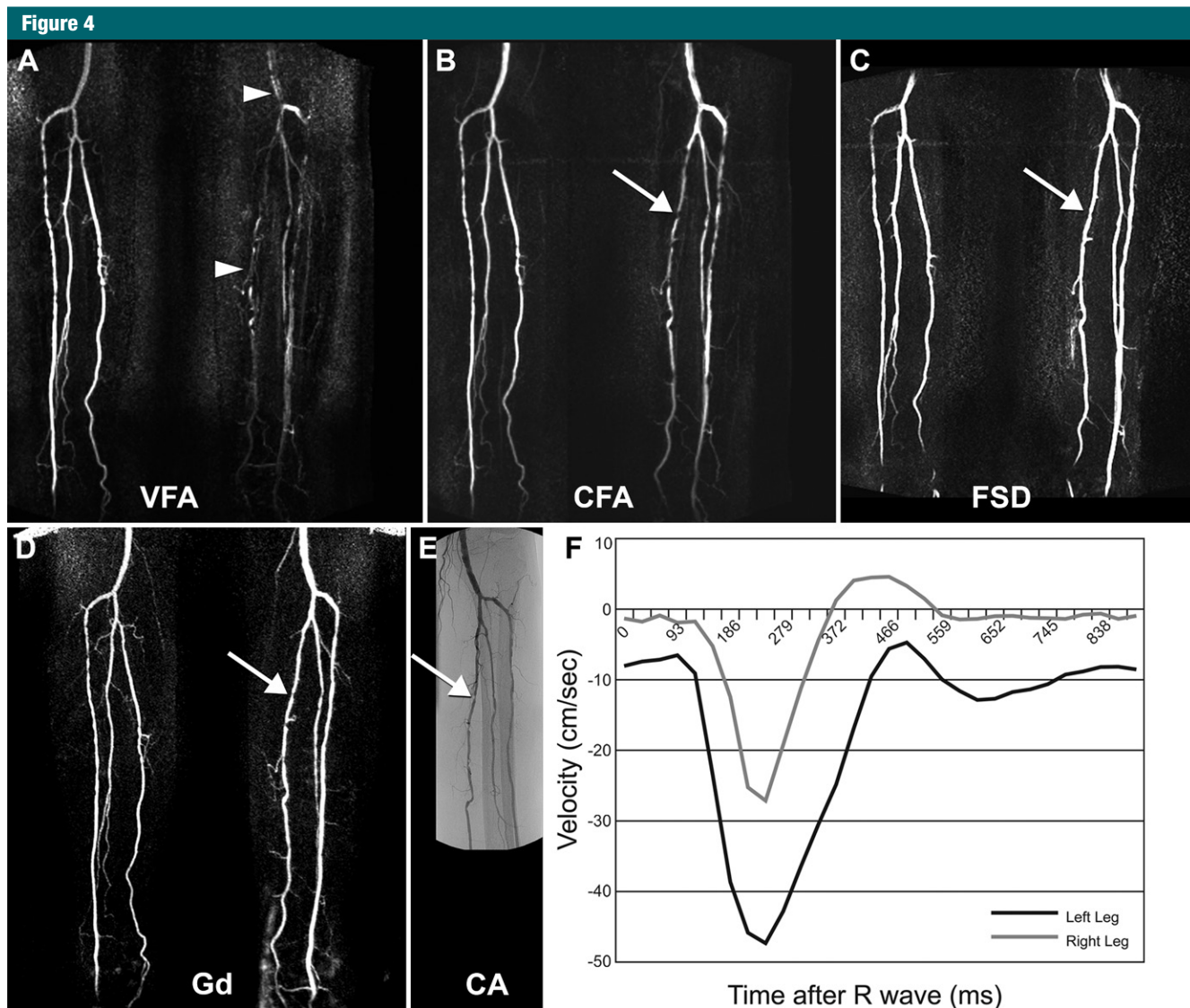


Figure 4: Foot ulcer of left leg in 73-year-old man with diabetes mellitus, with ABI of 1.0 in left leg and of 1.3 in right leg. *A*, Variable-FA (VFA) MR angiographic image. *B*, Constant-FA (CFA) MR angiographic image. *C*, FSD MR angiographic image. *D*, Time-resolved gadolinium (Gd)-enhanced MR angiographic image. *A–D*, Subtraction maximum intensity projection images. *E*, Conventional angiographic (CA) image depicts correlation of findings at proximal and middle areas of calf. For gadolinium-enhanced MR angiography, a fused image is provided; image of right leg was obtained at 64 seconds from commencement of time-resolved acquisition and image of left leg was obtained at 35 seconds from commencement of time-resolved acquisition, because of the differential rate of contrast enhancement between legs. A hemodynamically significant stenosis in the proximal left posterior tibial artery demonstrated at gadolinium-enhanced MR angiography and conventional angiography appears mildly overestimated at constant-FA MR angiography and underestimated at FSD MR angiography (arrow, *B*, *C*). Arteries of left calf are poorly visualized with variable-FA MR angiography (arrowheads, *A*) because of high diastolic arterial flow in left leg, as demonstrated in *F*. *F*, Phase-contrast velocity-time graph of posterior tibial arteries at midcalf level, where diastolic arterial velocity of left leg is approximately 8 cm/sec.

non-diagnostic image quality improved sensitivity and specificity of constant-FA MR angiography and variable-FA MR angiography.

FSD MR angiography, an SSFP-based technique, demonstrated good accuracy, was more robust to motion

because of background fat suppression, and was relatively unaffected by extremes of arterial flow. Diastolic FSD MR angiographic acquisitions depict bright blood regardless of velocity, as flow-sensitive dephasing preparation is not applied during diastolic acquisition,

and SSFP readout is inherently flow compensated (30). Systolic flow sensitivity was estimated a priori with the m_1 scout sequence and could be individually tailored and repeated for each leg at the expense of time. However, maximal craniocaudal coverage (400 mm) was

50 mm less than that of FSE MR angiography and gadolinium-enhanced MR angiography because of B_0 heterogeneity concerns, with implications for coverage in taller patients. FSD MR angiography sensitivity to B_0 heterogeneity could affect its utility with vascular stents (31) and with systems of greater than 1.5 T and/or short, wide-bore systems (32).

Combining constant-FA MR angiography and FSD MR angiography allowed achievement of greatest accuracy. With its robustness to arterial flow extremes, FSD MR angiography could be performed as the first-line nonenhanced calf MR angiographic technique at 1.5 T. Constant-FA MR angiography, with larger FOV and excellent NPV, could be supplementary for larger coverage or when B_0 inhomogeneity causes problems.

Limitations to our work include a relatively small patient group. The reader is advised to interpret results that are not significant with caution, as type II error may account for such results. Few patients had renal impairment; therefore, technique accuracy in patients with moderate to severe renal impairment who might receive greatest benefit was not specifically studied. A consensus interpretation of gadolinium-enhanced MR angiography was the reference standard, with intraoperative catheter angiography only available in a subset. At our institution, only patients in whom intervention is planned undergo conventional angiography. Further, use of a portable image intensifier and common femoral artery injections could decrease its accuracy.

While reader review of source diastolic images could have aided with un-evaluable segments for fast SE-based MR angiography (33), high background signal limited arterial conspicuity on source diastolic images. Time restrictions from multiple sequence comparisons meant full nonenhanced evaluation of the lower-extremity arteries from diaphragm to feet was not performed. We chose to target a particularly challenging region. Finally, statistical testing was performed without multiple comparison correction for optimal statistical power. Therefore, type I errors could potentially account

for reported significant results; results should be verified with a repeat study.

Future work includes accelerating nonenhanced MR angiography with compressed sensing to exploit MR angiographic sparsity and other refinements, to address patient motion, and to tailor imaging to each leg (34,35). For implementation as a true nonenhanced MR angiographic protocol, complete three-station evaluation is planned. Comparison with another large-coverage nonenhanced method, quiescent interval single-shot (or QISS) nonenhanced MR angiography, is warranted (24,36,37).

At 1.5 T, variable-FA and constant-FA fast SE-based MR angiography and FSD-prepared SSFP MR angiographic techniques demonstrate satisfactory image quality and excellent NPV for below-knee hemodynamically significant stenosis in a clinical population. They are a valuable alternative to gadolinium-enhanced MR angiography in patients with renal impairment or where intravenous access is a problem. FSD MR angiography is robust to arterial flow variations and can be performed first line at 1.5 T where exogenous contrast agents are undesirable or contraindicated. Constant-FA MR angiography could be complementary or could be a larger-coverage alternative if significant proximal disease is excluded.

Disclosures of Conflicts of Interest: R.P.L. No relevant conflicts of interest to disclose. Z.F. No relevant conflicts of interest to disclose. M.C. No relevant conflicts of interest to disclose. A.B. No relevant conflicts of interest to disclose. I.P.A. No relevant conflicts of interest to disclose. P.S. No relevant conflicts of interest to disclose. D.C.K. No relevant conflicts of interest to disclose. S.K. No relevant conflicts of interest to disclose. P.A.H. No relevant conflicts of interest to disclose. A.A. No relevant conflicts of interest to disclose. D.R.S. No relevant conflicts of interest to disclose. J.S.B. No relevant conflicts of interest to disclose. M.A.A. No relevant conflicts of interest to disclose. J.X. Financial activities related to the present article: none to disclose. Financial activities not related to the present article: employed by Siemens; author and institution have patents pending in the United States. Other relationships: none to disclose. D.L. No relevant conflicts of interest to disclose. V.S.L. Financial activities related to the present article: none to disclose. Financial activities not related to the present article: author and institution have patents pending in the United States. Other relationships: none to disclose.

References

- Rosamond W, Flegal K, Friday G, et al. Heart disease and stroke statistics: 2007 update—a report from the American Heart Association Statistics Committee and Stroke Statistics Subcommittee. *Circulation* 2007; 115(5):e69–e171.
- Andreisek G, Pfammatter T, Goepfert K, et al. Peripheral arteries in diabetic patients: standard bolus-chase and time-resolved MR angiography. *Radiology* 2007;242(2): 610–620.
- Koelemay MJ, Lijmer JG, Stoker J, Legemate DA, Bossuyt PM. Magnetic resonance angiography for the evaluation of lower extremity arterial disease: a meta-analysis. *JAMA* 2001;285(10):1338–1345.
- Met R, Bipat S, Legemate DA, Reekers JA, Koelemay MJ. Diagnostic performance of computed tomography angiography in peripheral arterial disease: a systematic review and meta-analysis. *JAMA* 2009;301(4): 415–424.
- Morasch MD, Collins J, Pereles FS, et al. Lower extremity stepping-table magnetic resonance angiography with multilevel contrast timing and segmented contrast infusion. *J Vasc Surg* 2003;37(1):62–71.
- Ouwendijk R, de Vries M, Stijnen T, et al. Multicenter randomized controlled trial of the costs and effects of noninvasive diagnostic imaging in patients with peripheral arterial disease: the DIPAD trial. *AJR Am J Roentgenol* 2008;190(5):1349–1357.
- Ouwendijk R, Kock MC, van Dijk LC, van Sambeek MR, Stijnen T, Hunink MG. Vessel wall calcifications at multi-detector row CT angiography in patients with peripheral arterial disease: effect on clinical utility and clinical predictors. *Radiology* 2006;241(2): 603–608.
- Murphy SW, Barrett BJ, Parfrey PS. Contrast nephropathy. *J Am Soc Nephrol* 2000;11(1):177–182.
- O'Hare AM, Bertenthal D, Shlipak MG, Sen S, Chren MM. Impact of renal insufficiency on mortality in advanced lower extremity peripheral arterial disease. *J Am Soc Nephrol* 2005;16(2):514–519.
- Grobner T. Gadolinium: a specific trigger for the development of nephrogenic fibrosing dermopathy and nephrogenic systemic fibrosis? *Nephrol Dial Transplant* 2006; 21(4):1104–1108.
- Sadowski EA, Bennett LK, Chan MR, et al. Nephrogenic systemic fibrosis: risk factors and incidence estimation. *Radiology* 2007; 243(1):148–157.

12. Fan Z, Sheehan J, Bi X, Liu X, Carr J, Li D. 3D noncontrast MR angiography of the distal lower extremities using flow-sensitive dephasing (FSD)-prepared balanced SSFP. *Magn Reson Med* 2009;62(6):1523–1532.
13. Miyazaki M, Takai H, Sugiura S, Wada H, Kuwahara R, Urata J. Peripheral MR angiography: separation of arteries from veins with flow-spoiled gradient pulses in electrocardiography-triggered three-dimensional half-Fourier fast spin-echo imaging. *Radiology* 2003;227(3):890–896.
14. Lim RP, Hecht EM, Xu J, et al. 3D nongadolinium-enhanced ECG-gated MRA of the distal lower extremities: preliminary clinical experience. *J Magn Reson Imaging* 2008;28(1):181–189.
15. Miyazaki M, Sugiura S, Tateishi F, Wada H, Kassai Y, Abe H. Non-contrast-enhanced MR angiography using 3D ECG-synchronized half-Fourier fast spin echo. *J Magn Reson Imaging* 2000;12(5):776–783.
16. Wedeen VJ, Meuli RA, Edelman RR, et al. Projective imaging of pulsatile flow with magnetic resonance. *Science* 1985;230(4728):946–948.
17. Storey P, Atanasova IP, Lim RP, et al. Tailoring the flow sensitivity of fast spin-echo sequences for noncontrast peripheral MR angiography. *Magn Reson Med* 2010;64(4):1098–1108.
18. Mugler JPI, Meyer H, Kiefer B. Practical implementation of optimized tissue-specific prescribed signal evolutions for improved turbo-spin-echo imaging [abstr]. In: Proceedings of the Eleventh Meeting of the International Society for Magnetic Resonance in Medicine. Berkeley, Calif: International Society for Magnetic Resonance in Medicine, 2003; 203.
19. Atanasova IP, Storey P, Lim RP, et al. Effect of flip angle evolution on flow sensitivities in ECG-gated fast spin echo MRA methods at 3T [abstr]. In: Proceedings of the Seventeenth Meeting of the International Society for Magnetic Resonance in Medicine. Berkeley, Calif: International Society for Magnetic Resonance in Medicine, 2009; 422.
20. Pomposelli FB, Kansal N, Hamdan AD, et al. A decade of experience with dorsalis pedis artery bypass: analysis of outcome in more than 1000 cases. *J Vasc Surg* 2003;37(2):307–315.
21. Lim RP, Jacob JS, Hecht EM, et al. Time-resolved lower extremity MRA with temporal interpolation and stochastic spiral trajectories: preliminary clinical experience. *J Magn Reson Imaging* 2010;31(3):663–672.
22. Fan Z, Zhou X, Bi X, Dharmakumar R, Carr JC, Li D. Determination of the optimal first-order gradient moment for flow-sensitive dephasing magnetization-prepared 3D non-contrast MR angiography. *Magn Reson Med* 2011;65(4):964–972.
23. Griswold MA, Jakob PM, Heidemann RM, et al. Generalized autocalibrating partially parallel acquisitions (GRAPPA). *Magn Reson Med* 2002;47(6):1202–1210.
24. Edelman RR, Sheehan JJ, Dunkle E, Schindler N, Carr J, Koktzoglou I. Quiescent-interval single-shot unenhanced magnetic resonance angiography of peripheral vascular disease: technical considerations and clinical feasibility. *Magn Reson Med* 2010;63(4):951–958.
25. Andersen CA. Noninvasive assessment of lower-extremity hemodynamics in individuals with diabetes mellitus. *J Am Podiatr Med Assoc* 2010;100(5):406–411.
26. Premalatha G, Ravikumar R, Sanjay R, Deepa R, Mohan V. Comparison of colour duplex ultrasound and ankle-brachial pressure index measurements in peripheral vascular disease in type 2 diabetic patients with foot infections. *J Assoc Physicians India* 2002;50:1240–1244.
27. Rutherford RB, Lowenstein DH, Klein MF. Combining segmental systolic pressures and plethysmography to diagnose arterial occlusive disease of the legs. *Am J Surg* 1979;138(2):211–218.
28. Kumar V, Abbas AK, Fausto N, Aster JC. Acute and chronic inflammation. In: Kumar V, Abbas AK, Fausto N, Aster JC, eds. *Robbins & Cotran pathologic basis of disease*. 8th ed. Philadelphia, Pa: Saunders, 2010; 43–78.
29. Storey P, Lim RP, Kim S, Stoffel DR, Lee VS. Arterial flow characteristics in the presence of vascular disease and implications for fast spin echo-based noncontrast MR angiography. *J Magn Reson Imaging* 2011; 34(6):1472–1479.
30. Bieri O, Scheffler K. Flow compensation in balanced SSFP sequences. *Magn Reson Med* 2005;54(4):901–907.
31. Bartels LW, Smits HF, Bakker CJ, Viergever MA. MR imaging of vascular stents: effects of susceptibility, flow, and radiofrequency eddy currents. *J Vasc Interv Radiol* 2001;12(3):365–371.
32. Rasmus M, Bremerich J, Egelhof T, Huegeli RW, Bongartz G, Bilecen D. Total-body contrast-enhanced MRA on a short, wide-bore 1.5-T system: intra-individual comparison of Gd-BOPTA and Gd-DOTA. *Eur Radiol* 2008;18(10):2265–2273.
33. Nakamura K, Miyazaki M, Kuroki K, Yamamoto A, Hiramane A, Admiraal-Behloul F. Noncontrast-enhanced peripheral MRA: technical optimization of flow-spoiled fresh blood imaging for screening peripheral arterial diseases. *Magn Reson Med* 2011;65(2):595–602.
34. Lustig M, Donoho D, Pauly JM. Sparse MRI: The application of compressed sensing for rapid MR imaging. *Magn Reson Med* 2007;58(6):1182–1195.
35. Atanasova I, Storey P, Kim D, Lim R, Lee V. ECG-gated fast spin echo MRA with interleaved acquisition of systolic and diastolic data for improved robustness to motion [abstr]. In: Proceedings of the Twentieth Meeting of the International Society for Magnetic Resonance in Medicine. Berkeley, Calif: International Society for Magnetic Resonance in Medicine, 2012; 3903.
36. Hodnett PA, Koktzoglou I, Davarpanah AH, et al. Evaluation of peripheral arterial disease with nonenhanced quiescent-interval single-shot MR angiography. *Radiology* 2011;260(1):282–293.
37. Hodnett PA, Ward EV, Davarpanah AH, et al. Peripheral arterial disease in a symptomatic diabetic population: prospective comparison of rapid unenhanced MR angiography (MRA) with contrast-enhanced MRA. *AJR Am J Roentgenol* 2011;197(6):1466–1473.